FINAL REPORT

Pilot Scale Assessment of a Deployable Photocatalytic Treatment System Modified with BiPO4 Catalyst Particles for PFAS Destruction in Investigation-Derived Wastewaters

SERDP Project ER18-1599

JANUARY 2020

Ezra Cates
Clemson University

SERDP
DOD ▪ EPA ▪ DOE

Page Intentionally Left Blank

Page Intentionally Left Blank

REPORT DOCUMENTATION PAGE

Form Approved
OMB No. 0704-0188

1. REPORT DATE *(DD-MM-YYYY)*	2. REPORT TYPE	3. DATES COVERED *(From - To)*
31/01/2020	SERDP Final Report	7/12/2018 - 7/12/2020

4. TITLE AND SUBTITLE
Pilot Scale Assessment of a Deployable Photocatalytic Treatment System Modified with BiPO4 Catalyst Particles for PFAS Destruction in Investigation-Derived Wastewaters

5a. CONTRACT NUMBER
18-C-0085

5b. GRANT NUMBER

5c. PROGRAM ELEMENT NUMBER

6. AUTHOR(S)
Ezra L. Cates

5d. PROJECT NUMBER
ER18-1599

5e. TASK NUMBER

5f. WORK UNIT NUMBER

7. PERFORMING ORGANIZATION NAME(S) AND ADDRESS(ES)
Clemson University
342 Computer Ct.
Clemson, SC 29625

8. PERFORMING ORGANIZATION REPORT NUMBER
ER18-1599

9. SPONSORING/MONITORING AGENCY NAME(S) AND ADDRESS(ES)
Strategic Environmental Research and Development Program
4800 Mark Center Drive, Suite 17D03
Alexandria, VA 22350-3605

10. SPONSOR/MONITOR'S ACRONYM(S)
SERDP

11. SPONSOR/MONITOR'S REPORT NUMBER(S)
ER18-1599

12. DISTRIBUTION/AVAILABILITY STATEMENT
DISTRIBUTION STATEMENT A. Approved for public release: distribution unlimited.

13. SUPPLEMENTARY NOTES

14. ABSTRACT

The BOHP/UV photocatalytic advanced oxidation process was developed at Clemson and previously shown via bench testing to rapidly mineralize PFOA in pure waters. The objectives of this limited scope project were to assess the capabilities of the treatment method for a wider range of PFAS contaminants relevant to IDW, identify important complex water matrix considerations and quenching species, and demonstrate performance of the catalyst upon incorporation into a deployable commercial photoreactor system. Furthermore, BOHP's lack of activity toward PFSAs warranted pursuit of a complimentary photocatalytic process to address this important subclass of PFAS contaminants. Photocatalytic reduction of PFOS by BiPO4 and GaOOH semiconductor particles was thus examined through bench experiments and one pilot test.

15. SUBJECT TERMS
PFAS; photocatalysis; bismuth phosphate; water treatment; groundwater; advanced oxidation

16. SECURITY CLASSIFICATION OF:			17. LIMITATION OF ABSTRACT	18. NUMBER OF PAGES	19a. NAME OF RESPONSIBLE PERSON
a. REPORT	b. ABSTRACT	c. THIS PAGE			Ezra L. Cates
UNCLASS	UNCLASS	UNCLASS	UNCLASS	40	19b. TELEPHONE NUMBER *(Include area code)* 919-210-2949

Page Intentionally Left Blank

Table of Contents

Tables

Figures

Acronyms

AFFF	aqueous film-forming foam		**LUMO**	lowest unoccupied molecular orbital
BOHP	bismuth oxyhydroxy phosphate ($Bi_3O[OH][PO_4]_3$)		**PFAS**	poly/perfluoroalkyl substances
C_0, high/low	initial concentration, high (53 ppm) or low (~100 ppb)		**PFBA**	perfluorobutanoic acid
Clemson-MUAL	Clemson multiuser analytical facility		**PFCA**	perfluorocarboxylic acids
DOC	dissolved organic carbon		**PFHxA**	perfluorohexanoic acid
e/h	electron-hole pair		**PFHpA**	perfluoroheptanoic acid
EDS	energy dispersive X-ray spectroscopy		**PFOA**	perfluorooctanoic acid
FTS	fluorotelomer sulfonate		**PFOS**	perfluorooctane sulfonate
GenX	2,3,3,3-tetrafluoro-2-(heptafluoropropoxy)propanoic acid		**PFPeA**	perfluoropentanoic acid
HOMO	highest occupied molecular orbital		**PFSA**	perfluorosulfonic acid
HPLC	high performance liquid chromatography		**SA**	surface area
IDW	investigation-derived wastewater		**SEM**	scanning electron microscopy
LC-MS/MS	liquid chromatography tandem mass spectrometry		**UV**	ultraviolet

Keywords

PFAS; photocatalysis; bismuth phosphate; water treatment; groundwater; advanced oxidation

Abstract

Introduction and Objectives. The BOHP/UV photocatalytic advanced oxidation process was developed at Clemson and previously shown via bench testing to rapidly mineralize PFOA in pure waters. The objectives of this limited scope project were to assess the capabilities of the treatment method for a wider range of PFAS contaminants relevant to IDW, identify important complex water matrix considerations and quenching species, and demonstrate performance of the catalyst upon incorporation into a deployable commercial photoreactor system. Furthermore, BOHP's lack of activity toward PFSAs warranted pursuit of a complimentary photocatalytic process to address this important subclass of PFAS contaminants. Photocatalytic reduction of PFOS by $BiPO_4$ and GaOOH semiconductor particles was thus examined through bench experiments and one pilot test.

Technical Approach. Semiconductor photocatalyst particles were synthesized in a hydrothermal reactor and suspended as slurries in UVC photoreactors. Degradation rates and intermediate products of select long- and short-chain PFCAs and GenX were assessed in pure and complex waters using HPLC and LC-MS/MS analyses. BOHP was further incorporated into a Purifics Photo-cat-L integrated pilot system with ceramic membrane catalyst recovery for comparison testing, and for treatment trials of IDW from two DoD sites. Reduction of PFOS using $BiPO_4$ and GaOOH catalysts was performed using bench reactors and additionally by treatment of the refractory component of the BOHP-treated effluent in the Photo-cat. Catalytic stability of the BOHP catalyst batch in the commercial reactor was monitored.

Results. In prepared water tests with the pilot system, BOHP/UV achieved >95% reduction of GenX and all PFCA parent compounds in under 20 min of irradiation time; however, treatment kinetics were slower than expected based on successful bench test results. Unlike degradation, mineralization rates correlated positively to chain length. In bench tests, co-present Cl^- and SO_4^{2-} were shown to slow PFOA degradation significantly, while natural organic matter had negligible impact on performance. Groundwater IDW showed successful removal of PFAS, though scale-up analysis showed that catalyst performance should be improved for adequate cost-viability. After 191 h of use in the pilot system, the single batch of BOHP showed no detectable decrease in catalytic activity, indicating robust operation. Proof-of-concept experiments for reductive degradation of PFOS were successful using $BiPO_4$ with methanol as an electron acceptor.

Benefits. The demonstrated performance of the BOHP/UV and $BiPO_4$/UV processes represent significant progress toward actualizing a comprehensive field-deployable system. Complete removal of PCFAs and other PFAS from real groundwater was successfully demonstrated in pilot tests, though energy input was deemed excessive. Follow-on research involving simple size reduction techniques for both BOHP and $BiPO_4$ catalyst particles is expected to drastically improve kinetics and allow cost-efficient operation. Additional work is needed to optimize reaction conditions for rapid PFOS degradation via reduction. Future catalyst improvements may be easily translated to field application by incorporation into existing Purifics Photo-cat models with design treatment rates up to 1 MGD.

1. Objectives

1.1 SERDP Relevance. As outlined in the ERSON-18-L1 Statement of Need, deployable treatment systems that achieve complete destruction of poly- and perfluoroalkyl substances (PFAS) are needed for treatment and discharge of DoD investigation-derived wastewaters. Advanced processes that mineralize PFAS completely to CO_2 and F^- products are most desirable, and a priority for technologies that are rapidly transferrable from laboratory concepts to practical full-scale systems is recognized. In this project, the technical merits of novel photocatalytic systems for PFAS destruction were assessed within the context of a pre-existing commercial hardware system (Purifics Photo-cat) sold by our industry partner.

1.2 Criteria for Success. Prior to this effort, bench-scale proof-of-concept of PFOA degradation and mineralization by UV-irradiated $Bi_3O(OH)(PO_4)_2$ particle suspensions (a.k.a. BOHP/UV) was demonstrated by the PI's group.[1] Success of this limited scope project criteria include: **(1)** demonstration of activity toward a wide range of additional long- and short-chain PFCAs and GenX; **(2)** demonstration of intermediate compound degradation and fluoride liberation; (3) identification of important quenching species in real water matrices and demonstration of efficacy using complex waters; **(4)** confirming BOHP catalyst stability and continued activity over week-long periods of operation; **(5)** predicted ability to reduce PFAS concentrations in IDW to below 70 ppt at 25 L/min process rates in full-scale units; and **(6)** proof-of-concept of PFOS degradation by a complimentary (add-on) photocatalytic reduction process. Research objectives were defined as follows:

Objective 1. Optimize an operational BOHP/UV photocatalytic pilot system by incorporating the catalyst into existing commercial packaged system (replacing the normal TiO_2 catalyst).

Objective 2. Obtain data on catalyst activity/degradation kinetics, impact of water constituents, catalyst stability, and overall system treatment efficiency for a range of PCFAs, perfluorosulfonic acids (PFSAs), and GenX, including the six PFAS compounds specified in the US-EPA UCMR-3.

Objective 3. Demonstrate IDW treatment using field samples from two DoD AFFF-contaminated sites.

Objective 4. Complete proof-of-concept bench-scale demonstration of PFOS degradation by a complimentary photocatalytic reduction process ($BiPO_4$/UV and/or GaOOH/UV).

2. Background

2.1 Photocatalytic Degradation of PFAS. Photocatalytic water treatment typically uses semiconductor nanoparticles in combination with UV irradiation to drive heterogeneous redox reactions. As seen in Fig. 1, photons having energies greater than the semiconductor's band gap energy (E_g) are absorbed to excite a valence band electron into the conduction band, resulting in a pair of charge carriers in the form of conduction band electrons (e^-_{cb}) and valence band holes (h^+_{vb}; collectively refered to herein as electron-hole pairs, *e/h*); these may react with water or dissolved molecules at the particle surface to result in reduction and oxidation, respectively. Photocatalytic

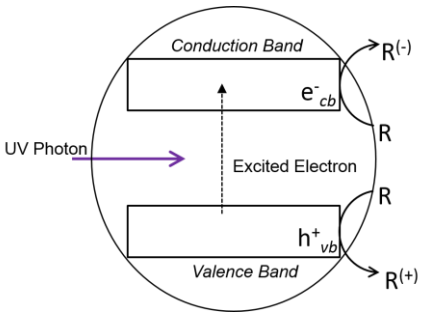

Figure 1. *Mechanism of heterogeneous photocatalytic oxidation/reduction by a semiconductor particle.*

processes are currently considered an ineffective treatment option for PFAS-contaminated water, though this sentiment may be attributed specifically to the common TiO_2/UV advanced oxidation process (AOP), which relies on oxidation of water to generate reactive •OH. Reduction potentials of •OH, or even photoexcited TiO_2 (2.9 V),[2] are not strong enough to oxidize PFAS. For example, PFOA has a reduction potential of 3.6 V.[3-6] Semiconductors with higher band gap energies are, however, capable of degrading PFAS under excitation by short wavelength UV (<320 nm).[4]

Limited data has been published on photocatalytic degradation of PFAS other than PFOA. Some investigations of intermediate compounds formed during PFOA degradation indicate that shorter-chain PFCAs were degraded, but the data do not allow accurate comparisons of relative degradation rates.[3, 7, 8] Furthermore, no published studies have demonstrated photocatalytic degradation of PFOS or GenX within practical timescales.

2.2 Properties of BOHP and $BiPO_4$. The photocatalytic activity of $BiPO_4$ was first revealed by Pan et al. in 2010, showing dye degradation twice as fast as P25 TiO_2, despite an order of magnitude lower surface area.[9] Its photoactivity was attributed to long photoexcited lifetime related to the ability of the PO_4^{3-} groups to attract h^+_{vb} and induce charge separation.[2] In 2017, the PI's group first achieved synthesis of a hydroxylated form of bismuth phosphate – $Bi_3O(OH)(PO_4)_2$ (BOHP).[1] *(This material was initially misidentified as a "mixed-phase $BiPO_4$ material", hence the use of this term in the original SERDP proposal.)* The composition and structure were a match to the naturally occurring mineral Petijeanite, which had not previously been studied as a photocatalyst.

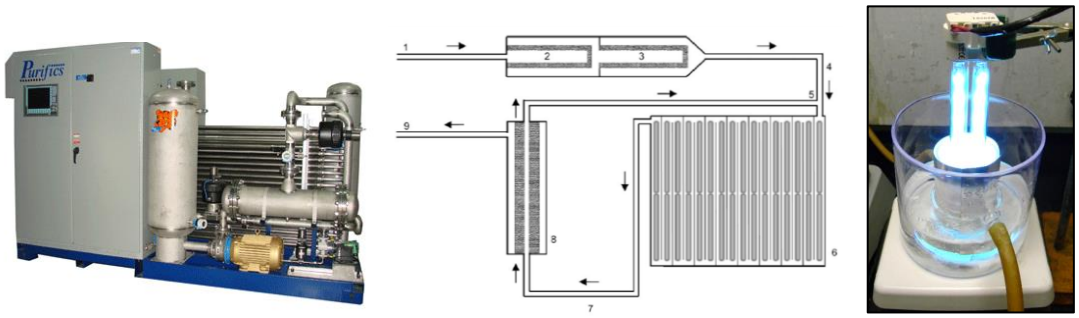

Figure 2. *(Left and center) Purifics Photo-cat 0.5 MGD TiO_2 slurry package system. indicating influent(1), bag filter(2), cartridge filter(3), influent sampling port(4), catalyst slurry addition(5), annular UV reactors(6), pre-membrane sampling port(7), ceramic membrane catalyst recovery system(8), and effluent(9). (Right) Bench-top immersion photoreactor used in this study.*

2.3 PFAS Degradation by BOHP. Preliminary results published by the PI's group in 2018 indicated that BOHP's positive surface charge imparted greater activity toward PFOA degradation compared to $BiPO_4$.[1] (For this reason, BOHP became the focus of most objectives of this project.) The point-of-zero charge was determined to be 5.9, and thus acidic conditions (pH ~4) encouraged favorable adsorption of PFOA anions to the BOHP surfaces and resulted in faster degradation and mineralization. The photocatalytic degradation rates of PFOA by BOHP in a bench reactor was compared to that by $BiPO_4$, Ga_2O_3, and TiO_2 in our previous work.[1] Under these conditions, degradation rates by BOHP far exceeded those of the reference catalysts, and kinetics were on the same order of magnitude as phenol degradation by TiO_2. Further details may be found in the publication. Lastly, degradation of PFOS by BOHP was also tested in the bench reactor, monitoring via fluoride release, and none was observed.[1]

2.4 Photocatalytic Reduction of PFOS. As stated above, BOHP/UV does not degrade PFOS under ambient oxidative conditions. Compared to PFCAs, PFOS has a higher HOMO-LUMO gap and is even more resistant to oxidation;[10] therefore, reductive strategies have been shown to be more successful.[11-13] Semiconductor photocatalysis can achieve reduction of target contaminants under reducing conditions that encourage direct heterogeneous reaction with e_{cb}^-. Therein, O_2 must be purged from the water to avoid e_{cb}^- scavenging, and an electron donor such as methanol should be added to react with h_{vb}^+ (see Fig. 1). Zhao et al. demonstrated that PFOA can be rapidly degraded via reduction by β-Ga_2O_3;[14] We previously tested PFOS degradation by β-Ga_2O_3 using the same method and failed to observed fluoride generation (unpublished). Thus no reports of PFOS photocatalytic reduction have been published.

2.5 Slurry-based Photocatalytic Treatment and the Purifics Photo-cat System. Slurry photocatalytic advanced oxidation water treatment proceeds by mixing catalyst particles with the influent at high concentrations (0.5-2 g/L) and passing the suspension in intimate contact with an array of UV lamps to induce redox reactions.[15] The main advantage therein is that high catalyst loading results in ample surface area for rapid contaminant destruction. While the slurry is opaque to UV and effectively self-shading, rapid mixing or turbulence can cycle water/catalyst in shaded areas closer to a lamp for activation. Catalyst particles must then be separated for reuse and to prevent contamination of the treated water. The Purifics Photo-cat® is a well-established brand of packaged slurry photocatalytic systems that has seen commercial success for small-scale wastewater, drinking water, and ex-situ groundwater treatment.[16] One of the models (0.5 MGD) is shown in Fig. 2. Influent is mixed with a catalyst slurry (typically P25 TiO_2) and pumped through an array of annular mercury lamp reactors in series. The annulus width is only 3 millimeters,[16] giving the suspension intimate contact with the lamps and confining turbulence within the irradiation zone. Catalyst recovery is achieved by ceramic crossflow ultrafiltration membranes with a cutoff size of 12 nm.[16] Compressed air injection is used to increase oxygenation and turbulence in the photoreactors, and to loosen particles from the membrane surface. Due to its use of TiO_2, the Photo-cat is not typically effective against PFAS due the poor efficacy of TiO_2 in degradation these compounds.[16] Since previous bench tests indicated PFOA was degraded by BOHP nearly as fast as typical organic contaminants were degraded by TiO2, it was hypothesized that BOHP could be used to treat PFAS in the Photo-cat platform with immediate "plug and play" field deployability.

3. Materials and Methods

3.1 Stock Chemicals and Syntheses. Stock chemical sources and purities are provided in the Appendix (Text A1). Preparation of BOHP micoparticle aggregates and n-$BiPO_4$ submicron particles was conducted according to previously published methods.[1] Larger batches of BOHP were synthesized using a 600 mL Parr Instruments hydrothermal reactor. Submicron GaOOH particles were also prepared via hydrothermal reaction, according to Muruganandham et al.[17] For structural, morphological, and electronic properties of these catalysts, the reader is referred to the works cited above.

3.2 Instrumental Analyses. Details of analytical methods are provided in the Appendix (Text A2). Degradation and mineralization of PFAS compounds during treatment experiments were monitored using several methods. For experiments concerning relative degradation rate comparisons of different PFAS and effects of water matrix anions, high initial PFAS concentrations (C_0) of 0.13 mM were used (*i.e.* 53 ppm for PFOA). Concentrations in these experiments were thus monitored using HPLC with UV detection. For experiments using low C_0

(10^2 ppb) in pure water or tap-water matrices, concentrations were monitored via LC-MS/MS at the Clemson Multiuser Analytical Lab (Clemson-MUAL). Analyses of untreated and treated IDW samples, for which a larger number of analytes were included, were conducted externally by Battelle Labs using LC-MS/MS. Additional analyses, including ion-exchange chromatographic determination of F^- concentrations, were conducted in the PI's lab and are described in the Appendix (Text A2).

3.3 Bench-top Photoreactor Experiments.

Bench Reactor. Small-scale photocatalytic treatments were conducted in a 280 mL cylindrical fused silica reactor vessel equipped with external anodized aluminum reflective jacket and magnetic stirring, and partially submerged in a flowing water bath to maintain room temperature conditions (Fig. 2). An 18 W compact fluorescent low pressure Hg lamp (254 nm) was submerged into the reactor in a pseudo-annular configuration. Additional details of the reactor and photocatalytic experimental procedure may be found in our previous work.[1] Adjustments of pH were achieved with NaCl/NaOH addition. The reactor and lamp were washed with tap water and then DI water between each experiment. We previously confirmed that the extent of adsorption of PFOA to the reactor vessel walls is negligible, as no significant removal was observed in control experiments using no addition of catalyst.[1] Conditions therein were the same as those used in bench reactor tests herein.

BOHP/UV Tests. For determination of degradation kinetics of PFCAs and GenX by BOHP/UV, initial suspension pH was adjusted to 4 unless stated otherwise. pH was not further adjusted during the experiments. Effects of various groundwater constituents on PFOA degradation were testing by adding NOM (humic substances), Cl^- (as NaCl), or SO_4^{2-} (as Na_2SO_4) to the suspensions prior to stirring in the dark. The effect of NOM was studied at low PFOA C_0, while anions were added to high C_0 suspensions. Acidification to pH 4 effectively removes all alkalinity, thus the effect of alkalinity was not studied.

$BiPO_4$/UV and GaOOH/UV Tests. Photocatalytic reduction of PFOS was assessed in the bench photoreactor using C_0=0.13 mM and $BiPO_4$ or GaOOH particles at 1.8 g/L. To induced reducing conditions, the suspension was bubbled with N_2 for 2 h in the dark, and then continuously purged during irradiation. Additionally, 12.3 mM of methanol was added to the suspension initially, and again every 2 h during irradiation. PFOS degradation was monitored indirectly via fluoride release and/or directly via LC-MS/MS.

3.4 Photo-cat Experiments. The Photo-cat-L system used herein contains 8 annular UVC photoreactors, each ~1 m long, containing 75 W low pressure mercury lamps made of high purity fused silica glass ("214 quartz") with sleeve of the same glass. Influent suspension is pumped through the reactors at 25 L/min to induce treatment, and then the catalyst is separated via ceramic membrane and recycled (Fig. 2). The system was operated in batch mode wherein effluent was recycled into the influent reservoir and then recombined with the catalyst slurry. A ceramic diffuser with gas injection port was used for optional purging of the influent with N_2. The system contains additional jackets around each lamp the enable optional cooling of the photoreactors during batch operation via a separate tap water cooling line. This cooling was employed herein, though the treatment water still had an elevated steady-state temperature of ~35 °C during experiments. Further hardware details of the Photo-cat-L may be found in Benotti et al.[18] and Gerrity et al.[19] A photograph if the unit is shown in Fig. A1 (Appendix).

Total volume of solution in the system was 16 L. Due to the relatively large volume maintained in the influent reservoir, the volume of the photoreactors was only 10.6% of the total volume (1.7 L); thus "operation time" was multiplied by 0.106 to show the "irradiation time", i.e.

the average time spent by the solution in the photoreactors. Degradation kinetics were plotted versus irradiation time, as this more accurately reflects the performance of a full-scale Photo-cat system which would have many more photoreactors in series and operate in flow-through mode.

Catalyst Loading. The original manufacturer's catalyst batch consisting of TiO_2 was drained from the system, followed by flushing with tap water. 20 g of BOHP was then added to the influent reservoir and dispersed within the slurry loop via pumping. The same procedure was used to replace BOHP with $BiPO_4$, though twice the flushing was used for this switch, as it was discovered that some TiO_2 remained after BOHP loading.

System flushing. Prior to experiments using high $C_{0,PFAS}$, the system was emptied of water while retaining the catalyst using the membrane, then filled with tap water and emptied again. These first two flushes, which typically contained PFAS from previous experiments, were collected as hazardous waste. Next, the system was flushed continuously with tap water while wasting down a drain for 30 min. Prior to experiments using low C_0, the system was flushed for 6 h.

Influent Loading. To load with influent and disperse PFAS homogeneously in the system, the washed unit was drained (with catalyst retained) and then 10 L of pre-mixed PFAS solution was added to the influent reservoir, and tap water was added to result in a final 16 L volume with desired C_0. Pumping was then initiated with UV lamps off to mix the system. This procedure was confirmed via HPLC to mix completely and result in a stable PFAS concentration at the effluent sampling port prior to engaging the UV lamps.

PFAS Degradation Tests. Degradation of PFAS by BOHP/UV in the Photo-cat system was tested using tap water matrix with PFAS spiked in the influent as described above. The pH was not adjusted because the tap water contained alkalinity and acidification would require excessive anion addition. Thus, initial pH for high-C_0 experiments was typically around 6.8, while the low-C_0 PFOA solution in tap water had initial pH of 7.3. Experiments monitoring PFOS degradation by $BiPO_4$/UV were conducted similarly, except high purity N_2 was injected. Methanol was also added at 12.3 mM to serve as an electron donor.

3.5 BOHP Stability Assessment. The photocatalytic activity of the BOHP was monitored primarily using dye degradation tests, to allow for fast analyses. After initially adding the fresh BOHP to the Photo-cat, blue food dye (McCormick) was mixed into the system. The lamps were initiated, and the degradation rate was monitored by taking samples from the effluent port and analyzing via UV/VIS spectroscopy to establish a reference dye degradation rate. Dye degradation rate by the BOHP batch was assessed once per month and compared to the reference rate. Additionally, PFOA degradation experiments also allowed periodic comparison the kinetics to earlier results.

Following completion of BOHP/UV experiments in the Photo-cat, the catalyst slurry was drained from the reactor. At that time the batch had been suspended in the system for 9 months, undergone 191 h of pumping in recycle mode, and 113 h with the lamps on. Samples of the particles were recovered via centrifugation and analyzed using SEM and EDS for comparison to the pristine material.

3.6 IDW Experiments. PFAS-contaminated IDW was received from two DoD sites: (1) Joint Base Naval Air Station Willow Grove, PA (BWMW15 cluster, 42 ft below surface) and (2) Former Wurtsmith Air Force Base, MI (collected on May 2 2019). For each IDW, 16 L (as received) were loaded into the Photo-cat and treated for 6 h (38 min irradiation) using BOHP/UV. Since water quality may have varied as pumping proceeded during collection, an equal amount of sample water (4 L) was taken from each of the 4 containers provided for each site and mixed in the Photo-cat to homogenize. As a result, initial concentrations for separate

experiments using the same site's water had some variation. General water quality parameters were also measured using the mixed water prior to treatment. Treated Photo-cat effluent from the IDW experiments was recovered and saved while the BOHP catalyst in the unit was replaced with $BiPO_4$. The water was then treated for an additional 6 h under reducing conditions to target the PFSAs assumed to remain after the first treatment step.

3.7. Scale-up analysis. Cost viability of applying the BOHP/UV process to full-scale treatment at IDW sites was performed on the basis of lamp energy used per volume of water treated ($kW \cdot h/m^3$) during testing as advised by engineers at Purifics, as follows:

$$E_t = \frac{n \times P_l \times t}{V}$$

Where E_t = treatment energy (kWh/m^3), n = number of UV lamps used during pilot test, P_l = power consumption of each lamp (kW), t = treatment time required to reduce target contaminant to acceptable discharge concentration during pilot test (h), and V = volume of the water treated during pilot test (m^3).

Multiplying by a desired full-scale flow rate gives the total required lamp wattage of the full-scale Photo-cat system:

$$P_{sys} = E_t \times Q$$

Where P_{sys} = total UV lamp power requirement of the full-scale treatment system (kW), and Q = target full-scale treatment rate (m^3/h).

The number of Photo-cat units needed (and capital cost) can then be determined by dividing P_{sys} by the total lamp power of the largest Photo-cat model, which is 141 kW.

4. Results and Discussion

4.1 Catalyst Syntheses. The structures, morphologies, and optical/electronic properties of the BOHP and $BiPO_4$ materials synthesized by these methods was described in our published works.[1, 20] Initial large-batch syntheses of BOHP in the 600 mL Parr reactor using stirring resulted in poor photocatalytic activity. Hydrothermal treatment of the precursor solution without stirring, however, result in BOHP particles which matched those of small-batch syntheses in terms of both morphology and PFOA degradation rate (data not shown).The XRD pattern and morphology (Fig. A2 in the Appendix) of synthesized GaOOH particles matched those of Muruganandham et al.[17] The yield, however, was prohibitively low at only 0.32 g per 600 mL reaction.

4.2 Bench-scale Assessment of PFAS Degradation by BOHP/UV in Prepared Waters.

Comparison of Degradation Rates Among Different PFAS. Degradation by BOHP/UV of a range of PFCAs were evaluated in bench photoreactors by direct addition at initial concentrations of 0.13 mM/53 ppm ("high C_0"), shown in Figure 3A. Longer chain length strongly correlated to faster degradation by BOHP/UV in the bench reactor, with C8-C10 compounds degrading rapidly, C7 (PFHpA) showing slow degradation, and C6 (PFHxA) and C5 (PFPeA) showing negligible degradation within 120 min. This trend can be explained by adsorption behavior, wherein longer-chain PFCAs adsorb more readily to surfaces [21, 22] and were degraded through direct reaction with BOHP *e/h* more rapidly. Adsorption was thus indicated as an important prerequisite for degradation in the bench photoreactor, as we previously reported in PFOA studies.[1] Acidic conditions result in positively charged BOHP surface, which encourages PFCA

adsorption via electrostatic attraction, followed by photocatalytic degradation. The effect was strongest for long-chain PFCAs which are more adsorbable; compounds of less than 7 carbons, however, have greater charge density and thus larger hydration shells that lend thermodynamic stability to the bulk aqueous phase.

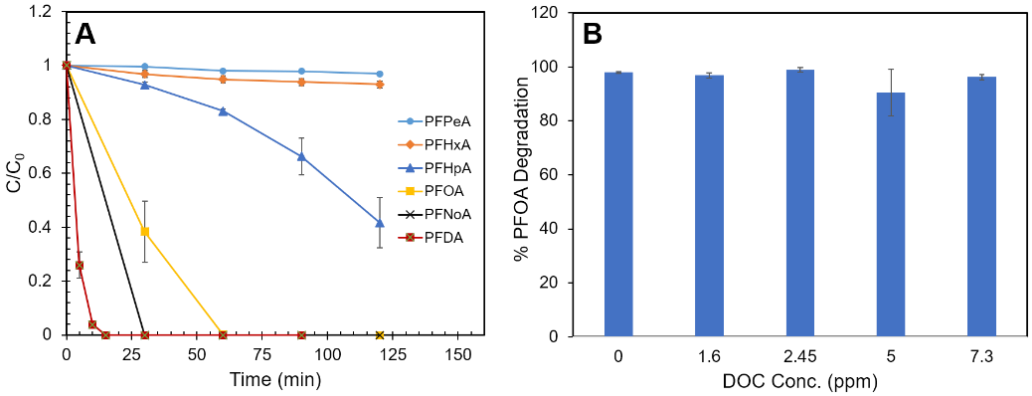

Figure 3. (A) *Degradation of PFCAs by BOHP/UV in bench-top photoreactors (C_0 = 53 ppm, pH_0 = 4).* ***(B)*** *Degradation percentage of PFOA at low C_0 (~100 ppb) in the presence of humic substances after 2 h irradiation in bench reactors (pH = 4). Initial equilibrium DOC concentrations following 2 h stirring in the dark are indicated on the x-axis. Error bars show standard deviations among 3 separate experiments.*

Effect of Groundwater Matrix Components. The effects of key groundwater co-constituents on PFOA degradation rates were assessed herein using benchtop photoreactors, including natural organic matter (NOM/humic substances; Suwanee River RO isolate), Cl^-, and SO_4^{2-}. In a previous publication we reported degradation of PFOA at 10^2 ppb-range initial concentration in the presence of 0.5 mg/L DOC by BOHP/UV.[1] The rate constant was 75% lower compared to PFOA degradation in pure water at ppm-range PFOA concentration, but it was unknown if this was due to the NOM or to the lower initial concentration of target compound. Figure 3B shows the percent of PFOA degradation (C_0 = 300 ppb) after 120 min of treatment in the bench reactors with NOM added at equilibrium concentrations up to 7.3 mg/L DOC. A similar decrease as before in degradation rate was observed compared to high C_0 tests. Interestingly, NOM concentration had no significant correlation to PFOA degradation rate, even at concentrations up to 24× that of PFOA initially. These data suggest that the slower kinetics were mainly a result of the low initial PFOA concentration and not the presence of NOM. Furthermore, the NOM itself was degraded by BOHP/UV with over 80% reduction in DOC at the highest initial concentration within the 120 min (Figure A3). The lack of any quenching effect on PFOA degradation may indicate that humic substances were degraded primarily by photocatalytically generated •OH in the bulk solution, and reacted minimally with BOHP h^+_{vb}. At pH 4, humic acids were protonated with no electrostatic attraction to the positively charged catalyst surface.

The effects of Cl^- and SO_4^{2-} at concentrations up to 100 ppm on PFOA degradation are shown in Figures 4A and 4B, respectively. The presence of both anions types negatively impacted PFOA degradation rate, with SO_4^{2-} having a greater impact on a per molar basis. Iguchi et al. conclusively showed that Cl^- was oxidized by the h^+_{vb} of layered double hydroxide photocatalysts to produce HOCl and thus acted as a hole quencher; given the wide band gap and oxidizing ability of BOHP, we speculate this is also the case, though confirmation is outside the scope of this work. Sulfate, on the other hand would not be oxidized further but likely acted by adsorbing to the BOHP surface; this in turn would neutralize positive surface charge and create a

potential barrier that interfered with the PFOA - h^{+}_{vb} direct reaction.[23] As seen in the data, the quenching effect begins to plateau at SO_4^{2-} concentrations greater than 20 ppm. Additional increases in SO_4^{2-} concentration resulted in a lesser increase in quenching, consistent with the catalyst surface approaching a saturated adsorption capacity.

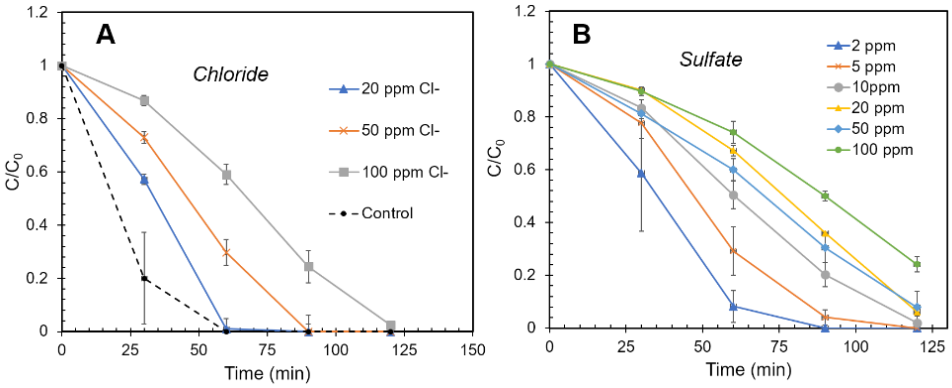

Figure 4. *PFOA degradation by BOHP/UV in the presence of* ***(A)*** *Cl^- and* ***(B)*** *SO_4^{2-} using bench photoreactors (pH_0 4, $C_{0,PFOA}$ = 53 ppm).*

4.3 Treatment of PFAS by BOHP/UV in Photo-cat System using Tap-water Matrix.

Comparison of Degradation and Mineralization Rates Among Different PFAS. Treatment of PFAS-contaminated water was assessed in the Photo-cat-L system containing BOHP. Tap water was used due the larger volume of the reactor and the need for multiple flushing steps between experiments; because the tap water contained an initial alkalinity of XX, acidification to pH 4 required more HCl addition and added potentially detrimental concentration of Cl^- to the system. A comparison test shown in Fig. 6A revealed that pH adjustment to 4 using HCl did not improve PFOA degradation in the Photo-cat at high C_0. Thus an even trade-off between favorable catalyst surface charge at low pH and inhibiting effect of added Cl^- was evident. Accordingly, PFCA degradation tests in the Photo-cat were conducted without acidification.

Degradation of long and short-chain PFCAs, as well as GenX, at high C_0 (0.13 mM) in a tap water matrix were evaluated using natural initial pH of 6.8-6.9. Water quality parameters of the employed tap water are shown in Table A1, including Cl^- and SO_4^{2-} concentrations of 7.7 and 10.8 ppm, respectively. The PFAS treatment results for the Photo-cat, shown in Figure 4A, do not display a correlation between PFCA chain length and degradation rate, in contrast to the bench reactor results. All PFCAs, as well as GenX, were degraded at similar rates with >95% removal in under 20 min of irradiation. A photolysis control test was also completed using the Photo-cat with no photocatalyst particles, resulting in only 17% PFOA degradation after 33 min irradiation, confirming the role of BOHP. (This minor PFOA degradation in the control test was attributed to photolysis incurred by the vacuum UV portion of the mercury lamp emissions.) Fluoride liberation data from the same experiments is shown in Figure 4B; in this case, a correlation to chain length was observed, with short-chain PFCAs mineralizing more slowly. Fluoride recovery corresponding to complete PFOA degradation was lower in the Photo-cat (46%) than in the bench reactors (63%)[1]. If we assume that the PFCA degradation products and pathways of BOHP/UV are similar in both reactor types, the lower F^- recovery of the Photo-cat could be due to greater loss of volatile fluorinated intermediates from the solution, such as trifluoroacetic acid. In recycle mode, the effluent return line cascades into the influent reservoir as a vortex that mixes aggressively with air and may have a significant air-stripping effect.

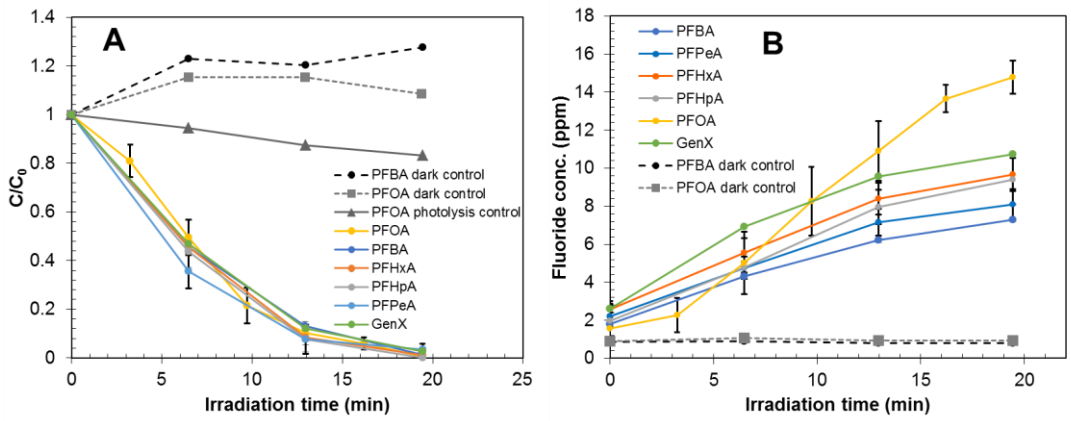

Figure 5. (A) *Degradation of PFCAs and GenX by BOHP/UV in the Photo-cat system (pH_0 ~6.8, $C_{0,PFAS}$ = 53 ppm).* ***(B)*** *Fluoride liberation during the same experiments. The 14.7 ppm F^- released during the PFOA experiment corresponds to 46% recovery.*

Discussion: Photocatalysis in Photo-cat System vs. Bench Reactors. Bench-top photoreactors were employed initially in this project to allow rapid experimentation and isolate optimum parameters without the intensive flushing steps required between controlled Photo-cat experiments. The behavior of BOHP/UV differed greatly between the two reactor types, however, in terms of relative degradation rates of different contaminants, and likely relative effects of quenching species as well. Photocatalytic efficacy in the bench reactors was strongly influenced by adsorption behavior, while the Photo-cat performance was not, which we attribute to the higher pH, differences in turbulence, and photoreactor configuration. At neutral pH, the catalyst surface was negatively charged, thus discouraging adsorption of long-chain PFCAs. Contaminant-catalyst contact in the Photo-cat thus relied on inertial collisions induced by stronger turbulence/velocity gradient. Theoretical root mean square velocity gradients were calculated to be on the order of 10^1 and 10^3 s^{-1} in the bench reactor and Photo-cat annuli, respectively. Higher velocity gradient results in higher rates of inertial collisions between catalyst particles and solutes in the water. Thus in the less turbulent bench reactors, PFAS that adsorbed well to the catalyst gained the intimate contact required for heterogeneous reaction, while those that adsorbed poorly did not. In the Photo-cat, however, we speculate that reactions following inertial collisions overshadowed the effects of adsorption and were of similar rates for all PFAS. Moreover, the narrow annulus width in the Photo-cat confined the entire velocity gradient distribution within a 3 mm irradiation channel which could be penetrated by UV. In the bench reactors, the highest velocity gradients occurred near the stir bar at the bottom, and more laminar-type flow occurred near the lamps where catalyst particles were irradiated. It is therefore concluded that a different bench reactor design is needed to simulate Photo-cat conditions within a smaller, more convenient volume. This reactor should use a similar annular configuration and flow-through mode with high pumping velocity, rather than a stirred, immersed lamp configuration.

Overall, PFCA degradation in the Photo-cat was slower than expected. Data provided by Purifics and verified by independent studies shows that degradation of typical organic contaminants by Photo-cat systems using TiO_2 require irradiation times of 1-2 min.[18, 19] Since our previous work showed that PFOA degradation by BOHP and phenol degradation by TiO_2 to proceed at roughly the same rates in our bench reactor,[1] we expected PFOA to also be degraded in ~1-2 min by BOHP in the Photo-cat. The use of tap water (containing Cl^- and SO_4^{2-}) and

neutral pH was likely responsible for the longer 18-20 min irradiation time required. Future testing of PFOA degradation in acidified pure water within the Photo-cat would be useful in deciphering the discrepancy between expected and observed performance. Contamination of this system with leftover TiO_2, described in a later section, may have also detracted from performance.

Treatment at Environmentally Relevant Concentrations. Degradation of PFOA in tap water matrix was also assessed at low C_0. First, in preliminary tests, flushing of the Photo-cat unit following high C_0 experiments was assessed to avoid excessive ppb-range carry-over contamination. Flushing data is provided in Table A2. PFOA degradation in tap water was conducted for 8 h of operation (53 min irradiation time) and samples were additionally monitored for PFCA intermediate compounds. Results, displayed in Fig. 6B, show that PFOA concentration dropped from 81 ppb to below detection limit (59 ppt) in less than 39 min of irradiation time. All intermediate PFCAs were degraded to below detection limits by 53 min, with the exception of PFHxA. The concentration of PFHxA peaked at 11 ppb at 6 min and had decreased to 190 ppt in the final sample; thus, it was approaching non-detect level as well.

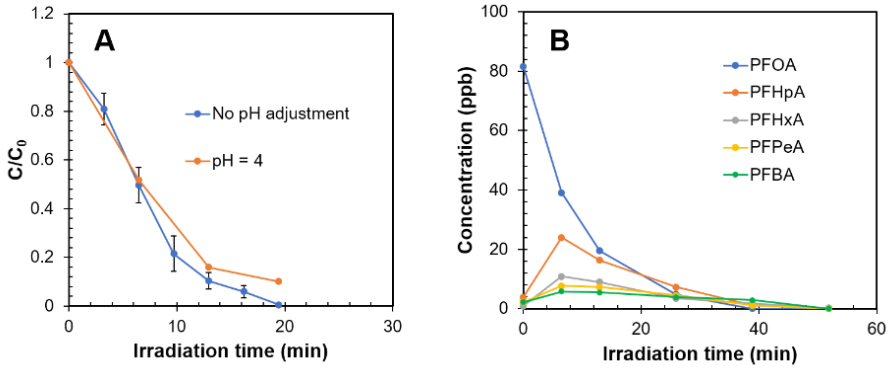

Figure 6. (A) *PFOA degradation (C_0 = 53 ppm) by BOHP/UV in tap water matrix in the Photo-cat system without acidification (pH_0 = 6.8) and with HCl addition (pH 4).* ***(B)*** *Concentrations of PFOA and intermediate PFCAs in tap water at environmentally relevant C_0 during BOHP/UV treatment in the Photo-cat.*

4.4 Treatment of IDW by BOHP/UV in Photo-cat system. General water quality parameters of the IDW samples employed are shown in Table A2. Of relevance to BOHP/UV, Wurtsmith water had relatively low levels of Cl^-, and SO_4^{2-} (< 6 ppm). Willow Grove water had elevated anion content including 19.9 ppm of Cl^- and 28 ppm of SO_4^{2-}.

Complete data on PFAS degradation results are provided in Table A4 and A5, and summarized here. Degradation of PFAS using BOHP/UV in the Photo-cat system was qualitatively similar for both IDW sites. Degradation was confirmed for C4-C10 PFCAs (Fig. 7A and C), while longer-chain PFCAs showed no observable degradation due to low initial concentrations (<10 ppt). Concentrations of some short-chain PFCAs increased initially before decreasing, indicating their generation within the system as byproducts of other PFAS being degraded. The magnitude of the increase in C4-C6 PFCAs during treatment of the Willow Grove water (Fig. 7C) suggests there were significant concentrations of other PFAS compound(s) beyond the 23 analytes studied herein being degraded to produce these intermediate concentrations. As expected, PFSAs were not degraded by BOHP/UV, however, fluorinated telomer sulfonates (6:2 and 8:2 FTS) were degraded by over 90% within 40 min (Table A4 and A5). Degradation of these compounds likely contributed to the significant formation of C4-C6 PFCAs intermediates in the Willow Grove water. Perfluorosulfonamide degradation was not observed, however, these compounds were detected at low initial concentration (~10 ppt). Dark control tests (Fig. 7A and D) confirmed that the observed reductions were due to primarily to photocatalytic degradation rather than adsorption with the system. The data at 13 min in Fig. 7B were possibly affected by contamination or improper dilution.

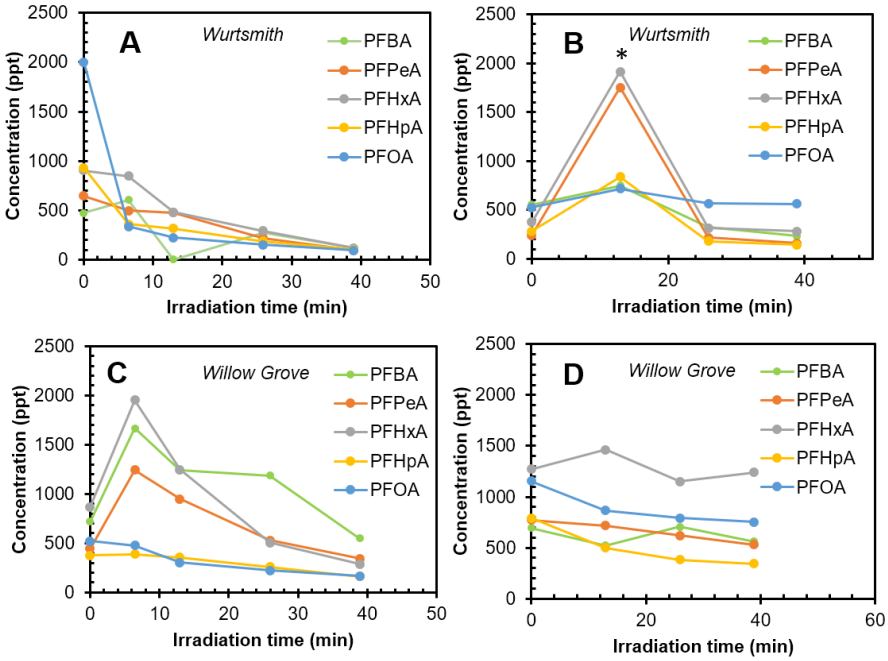

Figure 7. *Photocatalytic degradation* ***(A and C)*** *and dark control experiments* ***(B and D)*** *of PFCAs in IDW from Former Wurtsmith Airforce Base and Joint Naval Air Station at Willow Grove using the BOHP/UV process in a Photo-cat-L system. *Timepoint shows possible experimental error.*

PFOA concentrations were reduced from 2000 ppt to 98 ppt (95%) during 40 min irradiation of the Wurtsmith water, and from 521 ppt to 98 ppt (81%) in the Willow Grove water. The kinetics suggest that with extended irradiation time of ~60 min, the target concentration of <70 ppt could be attained for all PFCAs in the Wurtsmith water. In both cases the extent to which PFOA was concurrently produced as an intermediate of unknown PFAS degradation (and thus impacting apparent kinetics) was not known; however, the kinetics of degradation were

generally slower for the Willow Grove water, which may be attributed to its higher Cl^- and SO_4^{2-} content.

4.5 BOHP Stability Assessment and TiO_2 Contamination. Results of periodic dye degradation tests of the BOHP batch in the Photo-cat system are shown in Fig. 8. This same batch of catalyst was used for all BOHP Photo-cat experiments and endured 191 h of recirculation in the system. No change in dye degradation rate was observed over the 8-month timeframe, suggesting stable photocatalytic activity. No noticeable changes in PFOA degradation rate were noted either, throughout the course of the project. However, upon completion of BOHP experiments the catalyst slurry was drained from the system and its appearance had changed significantly compared to its original condition. When first prepared, it was an opaque white suspension containing micron-sized particle aggregates that settled rapidly in a beaker (<5 min). After recovery from the Photo-cat however, the particles were slightly discolored and consisted of a settleable portion, and a colloidal portion that did not settle.

Samples from both portions were dried and analyzed via SEM and EDS. SEM images of both portions are shown in Fig. A4, and reveal that the settleable portion resembles the original BOHP material, whereas the colloidal portion had smaller BOHP particles with an additional nanoparticulate component. Elemental analysis using EDS revealed that the nanoparticles were in fact TiO_2. It was concluded that the flushing procedure used to prepare the unit for BOHP addition was inadequate with respect to removal of the original manufacturer's catalyst material. We theorize that the presence of TiO_2 particles likely resulted in slower PFAS degradation kinetics during Photo-cat experiments, because TiO_2 particles intercepted UV photons and detracted from BOHP excitation. The extent to which kinetics were affected are unknown. Due to this discovery, the degree of system flushing prior to $BiPO_4$ experiments (described next) was increased to minimize contamination by BOHP or TiO_2 during $BiPO_4$ reductive treatment in the Photo-cat. Moreover, because TiO_2 can degrade the food dye indicator used to assess catalyst stability, its presence may have interfered with the BOHP stability assessment.

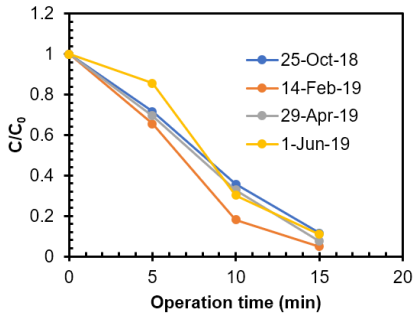

Figure 8. *Results of periodic dye degradation tests to confirm catalytic activity of the BOHP batch used in the Photo-cat.*

4.6 Scale-up Analysis. Based on results of IDW experiments, an irradiation time of 60 min (9.4 h of total operation time in the Photo-cat-L) was presumed to result in adequate treatment to <70 ppt for most PFCAs in a typical IDW. Table 1A shows results of scale-up analysis for a range of target treatment rates based on this value. Even a lower treatment rate of 25 L/min would require more than 3 full-scale Photo-cat units in series with a capital cost of roughly $1M each. Energy cost requirements for the UV lamps alone would exceed $35/m^3 at an electricity rate of $0.10/kWh. Current performance is thus unlikely to be cost effective, and at least a 10-fold enhancement in efficiency should be pursued. Results of scale-up analyes for such an enhancement is shown in Table 1B. Given additional research, this goal is realistically achievable, as described in Section 5.

Table 1. *Results of scale-up analyses based on performance results obtained in this study (A) and anticipated results after anticipated 10-fold enhancement in catalyst activity/process optimization (see section 5) (B). Values are estimates. Number of units is based on the largest available Photo-cat treatment system (141 kW).*

A	*Desired Treatment Rate*			**B**	*Desired Treatment Rate*		
L/min	25	250	379	L/min	25	250	379
gpm	6.6	66	100	gpm	6.6	66	100
Total power required (kW)	529	5288	8005		53	529	800
Number of Units Required	3.75	38	57		1	3.75	6
Capital cost estimate (million $)	3.75	38	57		1	3.75	6

4.7 Proof-of-concept: $BiPO_4$/UV and GaOOH/UV Photocatalytic Reduction of PFOS

$BiPO_4$/UV Bench Reactor Tests. Degradation results for water containing PFOS, PFOA, and PFBS (C_0 = 100 ppb for each, pH_0 = 7) by reductive $BiPO_4$/UV are shown in Fig. 9A. Both PFOS and PFOA displayed significant degradation, however, results were highly variable between replicates, and average degradation rates for both slowed after 2 h. The inconsistency was speculated to result from acidification that occurred, wherein pH dropped to <4 after 6 h for most experiments. Results of an additional set of experiments using only PFOS and monitoring fluoride release are shown in Fig. 9B, which confirm that mineralization rate becomes slower during the 6 h timeframe. The mechanism of photocatalytic degradation herein is not clear at this time; however, acidic conditions are generally considered detrimental to reductive processes, as H^+ can act as an electron scavenger. This notion was confirmed by conducting an additional PFOS mineralization test during which pH was readjusted to every 2 h using NaOH. Results (Fig. 9C) show a higher degree of fluoride liberation with more steady kinetics and faster mineralization when neutral pH was maintained. The 25 ppb F^- that appeared at 6 h for pH 7 condition corresponded to 39% fluoride recovery.

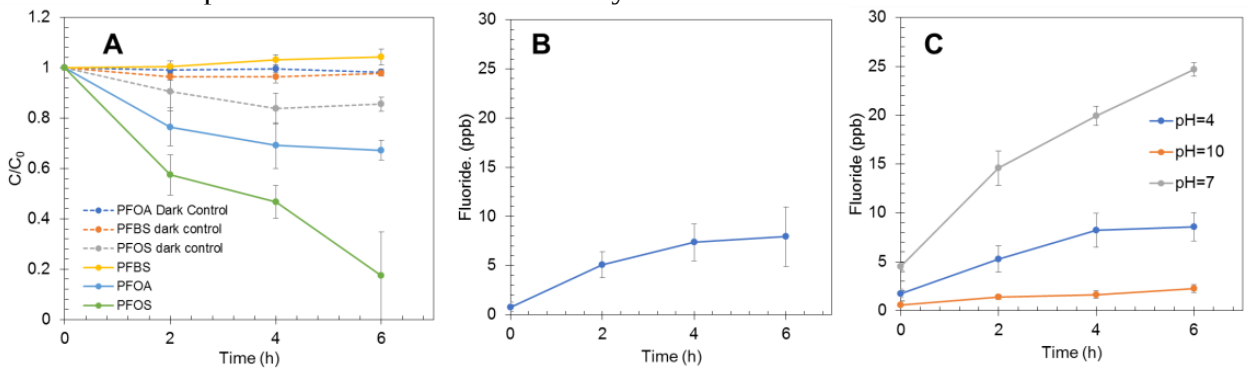

Figure 9. (A) *Degradation of PFOS, PFBS, and PFOA in mixed solution by $BiPO_4$/UV reductive treatment in the bench reactor with low C_0 (~100 ppb) and no pH readjustment.* ***(B)*** *Fluoride generation under the same conditions with only PFOS added (100 pb) and no pH adjustment.* ***(C)*** *Fluoride generation from PFOS degradation wherein pH was readjusted to the target value every 2 h.*

As seen in Fig. 9A, no decrease in PFBS concentration was observed during $BiPO_4$/UV treatment without pH readjustment; in fact, a slight increase was observed. PFBS was thus likely produced therein as a byproduct of PFOS degradation. Due to this interference, it remains unknown if PFBS can be degraded by $BiPO_4$/UV, but if so, it is likely inefficient under these conditions. Overall, degradation of PFOS by $BiPO_4$/UV was confirmed in the bench photoreactor, however, more extensive follow-up experiments are warranted to determine optimum conditions and reaction intermediates. Additionally, BOHP/UV research has revealed that adsorption is a key determinant of photocatalytic activity in the bench photoreactor, but not in the Photo-cat. Therefore, these results are of limited applicability to $BiPO_4$/UV performance in the Photo-cat.

Treatment of PFSA Component of IDW by $BiPO_4$/UV in Photo-cat System. Serving as a test of the $BiPO_4$/UV process in complex water matrices, treated effluent from the BOHP/UV process was used as influent for the reductive process experiment. As observed from the BOHP/UV Photo-cat data, the oxidative process did not degrade PFSAs; thus this water initially contained high concentrations of PFOS (10^2-10^4 ppt), with lower amounts PFCAs and short-chain PFSAs. Results of reductive $BiPO_4$/UV treatment in the Photo-cat unit are shown in Fig. 10 and were similar for both sites. For the Wurtsmith water, PFOS was reduced by 74% from an initial concentration of 765 ppt, while the Willow Grove water showed a 67% reduction from a C_0 of 9765 ppt, after 38 min of irradiation. Most short-chain PFSAs also showed minor reductions, however, these were possibly due to adsorption. The data do not suggest that short-chain PFSAs were formed as intermediates of PFOS degradation. PFCAs were also degraded by the

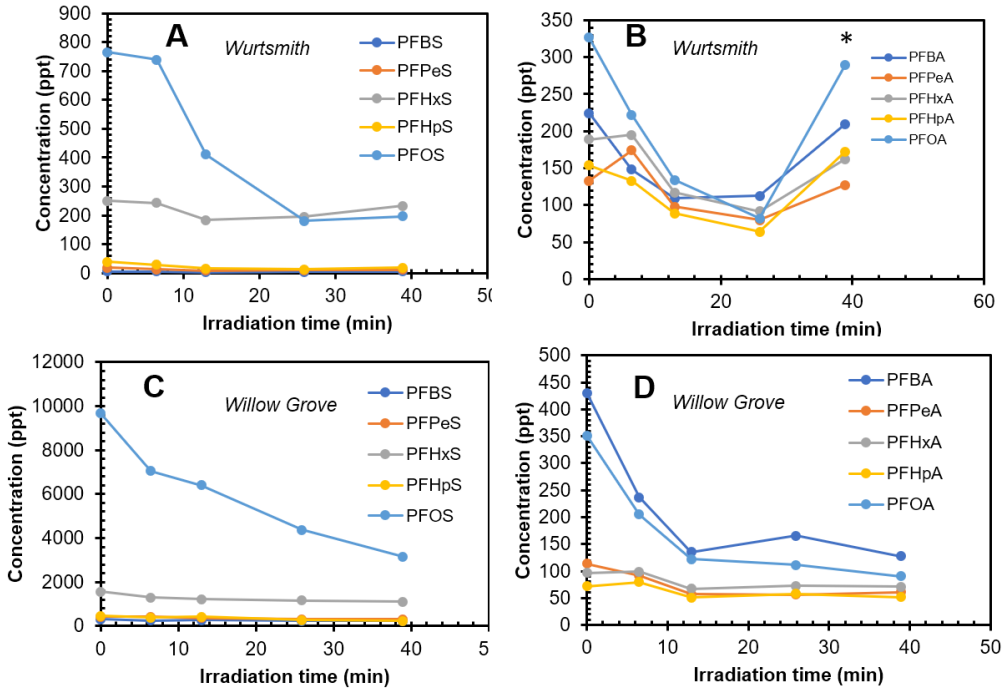

Figure 10. *Second stage photocatalytic treatment of IDW already treated by BOHP/UV, using the $BiPO_4$/UV photocatalytic reduction process in the Photo-cat, showing PFSA removal* ***(A and C)*** *and PFCA removal* ***(B and D)****.*

$BiPO_4$/UV process, albeit significantly slower than with oxidative BOHP/UV. The timepoint at 38 min (*) in Fig. 10B was deemed an outlier and the experiment should be repeated to gauge variability.

Due to aggressive mixing in the influent reservoir of the Photo-cat-L during batch mode operation, nitrogen purging was ineffective in removal dissolved O_2. The conditions employed were thus not truly reductive, and likely impacted performance to a great extent. The tests should be repeated using the aforementioned redesigned bench reactor with greater control over gas atmosphere. Reductive conditions are easily achievable in full-scale Photo-cat units, since they operate in flow-through mode and air is not remixed into the system. Further work is also needed to determine the degree to which co-present anions, particularly SO_4^{2-}, can quench the $BiPO_4$/UV process.

GaOOH/UV Tests. Existing research on GaOOH has reported highly favorable adsorption of PFOA and PFOS to GaOOH submicron particles,[17] and its band structure is also suitable for effective photocatalytic reduction based on our analysis. PFOS mineralization tests herein were inconclusive, however, as they were conducted prior to resolving an interference issue with ion chromatography analysis. Additionally, GaOOH particles were synthesized in the same hydrothermal reactors as bismuth catalyst and may have been contaminated by bismuth retained in the Teflon liners. Moreover, the synthesis method proved to have poor yield and it would not be practical to produce a batch that is large enough for the Photo-cat. It is thus advised that a bench-scale reactor of higher turbulence that matches the Photo-cat be developed in order to screen future catalysts that are difficult to synthesize in large batches according to existing methods. In conclusion, further work is needed to determine if GaOOH is a viable alternative to $BiPO_4$ for degrading PFSAs.

5. Conclusions and Implications for Future Research

5.1 Success Criteria Conclusions. All success criteria outlined in Section 1.2 were met, with the exception of criterion 5. While the BOHP/UV process was generally shown to be capable of degrading PFAS in IDW to below 70 ppt, it was not predicted be cost effective at full-scale without efficiency improvements. However, ample research avenues remain for improving efficiency to within cost-effective margins, which are outlined in the next section. Despite the one criterion not being met, the results of this project established valuable engineering guidelines for how an improved BOHP/UV process can be applied in the field. Effects of pH, anion content, NOM, were established, and the process was proven to degrade PFCAs, GenX, and FTSs. Proof-of concept PFOS degradation by reductive $BiPO_4$/UV was achieved as well, and new research objectives identified. Importantly, the robust operation of the Photo-cat system and stable photocatalytic activity of BOHP particles were confirmed. As described below, improved catalytic performance is likely achievable and the next catalyst embodiment may be easily incorporated in the Photo-cat system for rapid transfer from the lab to the field.

5.2 Future Research Directions.

BOHP/UV. Improving catalytic activity toward a 10-fold enhancement (or greater) in efficiency has been identified as the primary goal of follow-on research, with a time frame of 1 year. Foremost, smaller BOHP particles should be pursued in order to increase catalytic surface area (SA) by 10-20×. We previously measured the SA of BOHP to be only 2.5 m^2/g (compared to 57 m^2/g for TiO_2)[1, 24]. While this was not a limiting factor of photocatalytic performance in the bench reactors, it was likely highly limiting in the Photo-cat system. The high UV intensity and short exposure times in the annular photoreactors demand high catalyst surface area to allow

access of PFAS molecules to active sites at high rates. Ball milling, followed by mild annealing, may be used to reduce the BOHP particle sizes from several microns down to 10^1 nm for a 10-20× increase in specific SA. Improving SA of the catalyst is anticipated to result in a 5-15× enhancement in efficiency. Second, doping and defect chemistry strategies have been shown to enhance *e/h* separation and efficiency in $BiPO_4$ oxidative photocatalysis;[25-27] similar techniques applied to BOHP are likely to result in addition 50-100% enhancements in PFAS degradation rates.

Aside from catalyst modifications, process modifications should also be pursued to alleviate the observed discrepancy between BOHP's comparable PFCA degradation kinetics relative to normal TiO_2 photocatalysis in bench reactor, versus its much poorer relative performance in the Photo-cat system. Results herein revealed that due to the alkalinity of the tap water and IDW, pH could not be lowered to the desired value of 4 using HCl without adding detrimental concentrations of Cl^-. Thus the Photo-cat was operated a neutral pH that induced undesireable negative surface charge on BOHP (as studied in our previous work)[1]. While addition of H_2SO_4 or HNO_3 may also add anions that interfere photocatalysis, we expect the effect to be less severe, and gains in efficiency might be achieved by using such alternative acids to promote positively charge BOHP surfaces.

Lastly, the effect of TiO_2 contamination on the BOHP/UV process in the Photo-cat observed herein was not quantified. Enhanced efficiency will likely be observed when a pure BOHP suspension is employed.

$BiPO_4$/UV. Despite successful demonstration of PFOS degradation, the full potential of the reductive process was not revealed in this study. More effective purging of dissolved O_2 in the Photo-cat is needed, which may be achieved using a new bench reactor that mimics Photo-cat annulus conditions. This process may also be improved similarly to BOHP/UV described above using: smaller $BiPO_4$ particles, doping for improved *e/h* separation, and greater understanding of quenching by water co-constituents.

Comprehensive Photocatalytic PFAS Removal. Longer-term research may focus on how to combine oxidative and reductive processes for destruction of all PFAS in IDW. Methods of cycling between oxidative and reductive treatment for removal of both PFCAs and PFSAs are of interest. The full-scale Photo-cat systems are equipped with gas injections ports that allow control over dissolved O_2 concentrations at set points in the photoreactor train, and multiple approaches could be employed using Photo-cat units in series or switching oxidative/reducing conditions in the same unit. These include: BOHP(oxidation) → $BiPO_4$(reduction); $BiPO_4$(oxidation) → $BiPO_4$(reduction); and BOHP/$BiPO_4$(oxidation) → BOHP/$BiPO_4$(reduction), with the latter including either a mixture of the two catalyst particles or heterojunction particles containing both phases. While $BiPO_4$ has been shown to be less efficient at degrading PFCAs under oxidative conditions in a bench reactor,[1] the comparison test should be repeated under Photo-cat conditions.

Literature Cited

1. Sahu, S. P.; Qanbarzadeh, M.; Ateia, M.; Torkzadeh, H.; Maroli, A. S.; Cates, E. L., Rapid Degradation and Mineralization of Perfluorooctanoic Acid by a New Petitjeanite $Bi_3O(OH)(PO_4)_2$ Microparticle Ultraviolet Photocatalyst. *Environmental Science & Technology Letters* **2018,** *5*, (8), 533-538.
2. Pan, C.; Zhu, Y., A review of BiPO4, a highly efficient oxyacid-type photocatalyst, used for environmental applications. *Catalysis Science & Technology* **2015,** *5*, (6), 3071-3083.
3. Li, X.; Zhang, P.; Jin, L.; Shao, T.; Li, Z.; Cao, J., Efficient Photocatalytic Decomposition of Perfluorooctanoic Acid by Indium Oxide and Its Mechanism. *Environmental Science & Technology* **2012,** *46*, (10), 5528-5534.
4. Shao, T.; Zhang, P.; Jin, L.; Li, Z., Photocatalytic decomposition of perfluorooctanoic acid in pure water and sewage water by nanostructured gallium oxide. *Applied Catalysis B: Environmental* **2013,** *142–143*, 654-661.
5. Merino, N.; Qu, Y.; Deeb, R. A.; Hawley, E. L.; Hoffmann, M. R.; Mahendra, S., Degradation and Removal Methods for Perfluoroalkyl and Polyfluoroalkyl Substances in Water. *Environmental Engineering Science* **2016,** *33*, (9), 615-649.
6. Lin, H.; Niu, J.; Ding, S.; Zhang, L., Electrochemical degradation of perfluorooctanoic acid (PFOA) by Ti/SnO_2–Sb, Ti/SnO_2–Sb/PbO_2 and Ti/SnO_2–Sb/MnO_2 anodes. *Water Research* **2012,** *46*, (7), 2281-2289.
7. Zhao, B.; Zhang, P., Photocatalytic decomposition of perfluorooctanoic acid with β-Ga_2O_3 wide bandgap photocatalyst. *Catalysis Communications* **2009,** *10*, (8), 1184-1187.
8. Xu, J.; Wu, M.; Yang, J.; Wang, Z.; Chen, M.; Teng, F., Efficient photocatalytic degradation of perfluorooctanoic acid by a wide band gap p-block metal oxyhydroxide InOOH. *Applied Surface Science* **2017,** *416*, 587-592.
9. Pan, C.; Zhu, Y., New Type of $BiPO_4$ Oxy-Acid Salt Photocatalyst with High Photocatalytic Activity on Degradation of Dye. *Environmental Science & Technology* **2010,** *44*, (14), 5570-5574.
10. Torres, F. J.; Ochoa-Herrera, V.; Blowers, P.; Sierra-Alvarez, R., Ab initio study of the structural, electronic, and thermodynamic properties of linear perfluorooctane sulfonate (PFOS) and its branched isomers. *Chemosphere* **2009,** *76*, (8), 1143-1149.
11. Sun, Z.; Zhang, C.; Chen, P.; Zhou, Q.; Hoffmann, M. R., Impact of humic acid on the photoreductive degradation of perfluorooctane sulfonate (PFOS) by UV/Iodide process. *Water Research* **2017,** *127*, 50-58.
12. Song, Z.; Tang, H.; Wang, N.; Zhu, L., Reductive defluorination of perfluorooctanoic acid by hydrated electrons in a sulfite-mediated UV photochemical system. *Journal of Hazardous Materials* **2013,** *262*, 332-338.
13. Gu, Y.; Dong, W.; Luo, C.; Liu, T., Efficient Reductive Decomposition of Perfluorooctanesulfonate in a High Photon Flux UV/Sulfite System. *Environmental Science & Technology* **2016,** *50*, (19), 10554-10561.
14. Zhao, B.; Lv, M.; Zhou, L., Photocatalytic degradation of perfluorooctanoic acid with β-Ga_2O_3 in anoxic aqueous solution. *Journal of Environmental Sciences* **2012,** *24*, (4), 774-780.
15. Crittenden, J. C.; Trussell, R. R.; Hand, D. W.; Howe, K. J.; Tchobanoglous, G., *Water Treatment Principles and Design*. John Wiley & Sons: 2012.
16. Purifics-Inc., Technology Briefing: Photo-cat Multi-barrier Water Purification. In 2009.
17. Muruganandham, M.; Suri, R. P. S.; Abdel Wahed, M. S. M.; Sillanpää, M.; Wu, J. J.; Ahmmad, B., Synthesis, Characterization of alpha-GaOOH Self-Assembly and Its Application in Removal of Perfluorinated Compounds. *Journal of Nanoscience and Nanotechnology* **2015,** *15*, (9), 6524-6532.
18. Benotti, M. J.; Stanford, B. D.; Wert, E. C.; Snyder, S. A., Evaluation of a photocatalytic reactor membrane pilot system for the removal of pharmaceuticals and endocrine disrupting compounds from water. *Water Research* **2009,** *43*, (6), 1513-1522.

19. Gerrity, D.; Ryu, H.; Crittenden, J.; Abbaszadegan, M., Photocatalytic inactivation of viruses using titanium dioxide nanoparticles and low-pressure UV light. *Journal of Environmental Science and Health, Part A* **2008,** *43*, (11), 1261-1270.
20. Sahu, S. P.; Cates, E. L., X-ray Radiocatalytic Activity and Mechanisms of Bismuth Complex Oxides. *The Journal of Physical Chemistry C* **2017,** *121*, (19), 10538-10545.
21. Higgins, C. P.; Luthy, R. G., Sorption of Perfluorinated Surfactants on Sediments. *Environmental Science & Technology* **2006,** *40*, (23), 7251-7256.
22. Du, Z.; Deng, S.; Bei, Y.; Huang, Q.; Wang, B.; Huang, J.; Yu, G., Adsorption behavior and mechanism of perfluorinated compounds on various adsorbents—A review. *Journal of Hazardous Materials* **2014,** *274*, 443-454.
23. Abdullah, M.; Low, G. K. C.; Matthews, R. W., Effects of common inorganic anions on rates of photocatalytic oxidation of organic carbon over illuminated titanium dioxide. **1990**.
24. Suttiponparnit, K.; Jiang, J.; Sahu, M.; Suvachittanont, S.; Charinpanitkul, T.; Biswas, P., Role of Surface Area, Primary Particle Size, and Crystal Phase on Titanium Dioxide Nanoparticle Dispersion Properties. *Nanoscale Res Lett* **2011,** *6*, (1), 27-27.
25. Huang, H.; Qi, H.; He, Y.; Tian, N.; Zhang, Y., Enhanced photocatalytic activity of Eu^{3+}- and Gd^{3+}-doped BiPO4. *Journal of Materials Research* **2013,** *28*, (21), 2977-2984.
26. Pan, C.; Xu, J.; Chen, Y.; Zhu, Y., Influence of OH-related defects on the performances of $BiPO_4$ photocatalyst for the degradation of rhodamine B. *Applied Catalysis B: Environmental* **2012,** *115–116*, 314-319.
27. Lv, Y.; Zhu, Y.; Zhu, Y., Enhanced Photocatalytic Performance for the $BiPO_{4-x}$ Nanorod Induced by Surface Oxygen Vacancy. *The Journal of Physical Chemistry C* **2013,** *117*, (36), 18520-18528.

Appendix

Supporting Text

Text A1. Materials. Perfluorodecanoic acid (PFDA, 98%)\, perfluorononanoic acid (PFNA, 99%), perfluorooctanoic acid (PFOA, 96%), perfluoroheptanoic acid (PFHpA, 99%), perfluorobutanoic acid (PFBA, 98%) and bismuth nitrate (pentahydrate, 99.99%) were purchased from Aldrich. Perfluorohexanoic acid (PFHxA), perfluoropentanoic acid (PFPeA, 97%) and ammonium dihydrogen phosphate (99.99%) were supplied from Oakwood Chemicals, Alfa Aesar and Acros Organics respectively. High purity ammonium acetate powder was used to prepare mobile phase along with HPLC grade methanol, both obtained from Fisher Chemicals. The natural organic matter used in this study was RO isolated Suwanee River supplied from the International Humic substances Society. Ultra-high purity oxygen and high-purity nitrogen tanks were supplied from Airgas.

Text A2. Characterizations and Analyses. Catalyst particle characterization via XRD, SEM, and EDS were conducted using instrumentation described previously.[1]

PFAS analyses in the experiments with high initial concentrations of PFCAs in pure water used an Ultimate 3000 high performance liquid chromatography (HPLC) system (Thermo Scientific) consisting of an automatic sampler, a separation column (Zorbax SB C-18, 2.1 mm i.d., 150 mm length, 3.5 μm pore size) and UV-Vis detector was used to quantify the concentration of remaining PFCA in the solution. An isocratic elution with methanol and ammonium acetate (20 mM) as mobile phases were used at the flow rate of 0.4 mL/min. Different eluent ratios were used to detect each PFCA; PFOA-70:30 (v/v), PFNA-75:25, PFHpA-65:35, PFHxA-60:40, PFPeA-55:45, PFBA- 50:50. A 5 point linear calibration with an r^2>0.99 was prepared for each analyte. All the experiments were repeated in triplicate and analyzed, unless elsewhere mentioned. As the in-house measurements using HPLC were used only to assess kinetics (C/C_0) for each analyte, no external QC standards were used. Calibration curves are shown in Figure A5.

The concentrations of fluoride and other anions were determined using ICS-2100 ion chromatography system coupled with a Dionex IonPac AS9-HC column (4 × 250 mm) equipped with a conductivity detector, using 9 mM Na_2CO_3 as the mobile phase at a flow rate of 1 mL/min and NaF as a calibration standard.

Quantifications of PFAS during low concentration experiments were conducted by the Clemson Multiuser Analytical Lab using LC-MS/MS. They provided the following method description: A Shimadzu Prominence UFLC coupled to ESI-triple quadrupole (Shimadzu LCMS 8040) operated in the negative ionization mode. Chromatographic separation of PFAS from aqueous matrices was carried out on a reversed-phase UPLC Synergi Polar C18 4.6 mm × 250 mm, 4.0-μm column. Gradient elution was performed with 100% water containing 10 mmol/L ammonium formate for solvent A and 100% acetonitrile as solvent B. The flow-rate used was 0.6 mL/min and gradient conditions consisted of: 0 min: 10% B, 2 min: 10% B, 12 min: 40% B, 22 min: 95% B, 28 min: 95% B, 28.01 min: 10% B, and 35 min: 10% B. Sample injection volumes

ranged between 30 µL and 100 µL. For increased sensitivity and selectivity of the tested PFASs, data acquisition was performed in Multiple Reaction Monitoring (MRM) modes. The ion-spray potential for ESI was set to -3.5 kV. Nitrogen was used as nebulizing gas (12 L/min) and argon was employed as the collision gas. The source DL temperature was set to 250 °C and the heat block was set to 400 °C. The optimized settings for collision energy (CE), dwell time, as well as Q1 and Q3 Pre Bias potentials were tested for each target analyte by flow-injection analysis. The most abundant ion was chosen as the primary precursor ion and the first transition, which corresponds to the most abundant product ion was used for quantification. The second transition was used for confirmation purposes except for those with only one transition. For quantification of PFOA at high concentrations (>2000 ng/L), low-volume (5 µL) direct injection was performed. For quantification of PFAS at low concentrations (<2000 ng/L), high-volume (100 µL) direct injection was performed. Calibration curves were constructed for all target analytes by injecting matrix-matched calibration standards directly into the UPLC using standards. For simultaneous quantification and confirmation purposes, two MRM transitions were used to avoid false negatives at trace levels.

For experiments using IDW, PFAS analyses were conducted by Battelle Labs, who provided the following method description: PFAS compounds were extracted and prepared for analysis utilizing the appropriate technique dependent on matrix. The extracts were analyzed by LC-MS/MS monitoring the primary transition for each target analyte, when available, a secondary transition is monitored for confirmation. The analytes were identified by the primary transition and retention time. The identified analytes are quantified using an isotopic dilution approach (where an isotopically labelled compound was not available for a target analyte, the labelled analog with the closet retention time (RT) is used for quantification). A data system interfaced to the LC-MS/MS is used to control acquisition and to store, retrieve, and manipulate LC-MS/MS data. A 5-point linear fit calibration (6-point is quadratic curve fit used), with labeled analyte concentrations between 70% and 130% of true value and an r^2>0.99. Example calibration data is provided in Figure A6. ICC (Independent Calibration Check) must have the individual analyte %DIFF < 30%, with labeled analyte concentrations between 70% and 130% of true value, and IS area +/- 50% of L5 of ICAL. CCV (Continuing Calibration Check) every 10 samples with the individual analyte %DIFF < 30%, with labeled analyte concentrations between 70% and 130% of true value. Procedural blank and laboratory control samples were performed for all analyses.

Supporting Tables

Table A1. Tap water parameters.

	Concentration (ppm unless noted)
TOC	0.782459
Chloride	7.725
Nitrite	below D.L. (50 ppb)
Bromide	0.068
Nitrate	0.14
Phosphate	0.118
Sulfate	10.812
Fluoride	0.43
pH	7.38
Alkalinity (as CaCO3)	12.8 mg/L
UV transmittance (254 nm)	97.95%

Table A2. Results of Photo-cat flushing test following high-C_0 experiments.

Flushing time	PFOA concentration (ppb)
0h	64.926
2h	31.698
4h	0.662
6h	0.423

Table A3. Initial water quality contents of IDW samples employed.

	Wurtsmith	**Willow Grove**
Chloride (ppm)	1.66	19.9
Nitrate (ppm)	1.56	2.85
Sulfate (ppm)	5.54	28.14
Fluoride (ppb)	41.7	78.08
TOC (mg C/L	1.900546	0.837
pH	7.63	7.4
Alkalinity (mg/L $CaCO_3$)	104	120
UVT_{254} (%)	87.32%	94.96%

Table A4. PFAS data from BOHP/UV Treatment of IDW from Former Wurtsmith Site (Units: ppt)

Irradiation Time (min)	**0.00**	**6.48**	**12.96**	**25.92**	**38.88**
PFBA	473.94	605.27	3.05	274.39	120.21
PFPeA	648.18	497.19	478.23	222.53	95.86
PFHxA	905.60	847.83	483.15	292.40	120.37
PFHpA	932.44	362.91	318.29	188.52	106.06
PFOA	1999.64	336.84	226.80	152.04	98.44
PFNA	15.29	19.35	18.93	11.71	8.73
PFDA	11.17	8.17	9.81	7.16	4.51
PFUnA	5.56	5.56	6.10	6.10	5.43
PFDoA	2.78	2.78	3.05	3.05	2.72
PFTrDA	2.78	2.78	3.05	3.05	2.72
PFTeDA	5.56	5.56	6.10	6.10	5.43
NMeFOSAA	11.11	11.11	12.20	12.20	10.87
NEtFOSAA	5.56	5.56	6.10	6.10	5.43
PFBS	8.47	9.31	9.94	9.39	9.89
PFPeS	32.39	27.18	31.31	26.47	28.97
PFHxS	545.94	506.47	594.91	585.28	598.54
PFHpS	127.41	64.19	64.97	75.95	72.49
PFOS	1707.32	1846.28	2151.66	1731.19	2025.52
PFNS	5.56	5.56	6.10	6.10	5.43
PFDS	2.78	2.78	3.05	3.05	2.72
4:2FTS	3.22	2.73	3.05	3.05	2.72
6:2FTS	282.74	134.15	15.47	15.24	13.59
8:2FTS	48.10	13.79	2.36	3.05	2.72

Table A5. PFAS data from BOHP/UV Treatment of IDW from Willow Grove Site (Units: ppt)

Irradiation Time (min)	**0.00**	**6.48**	**12.96**	**25.92**	**38.88**
PFBA	717.80	1666.59	1240.03	1185.02	547.57
PFPeA	444.87	1242.90	947.57	527.47	345.56
PFHxA	869.45	1951.80	1247.28	505.65	286.94
PFHpA	376.57	388.60	356.55	259.34	163.78
PFOA	521.42	475.34	303.50	221.19	164.99
PFNA	10.27	13.55	14.87	10.81	6.86
PFDA	5.39	5.35	5.10	4.52	2.94
PFUnA	4.90	4.90	4.81	4.90	5.21
PFDoA	2.45	2.45	2.40	2.45	2.60
PFTrDA	2.45	2.45	2.40	2.45	2.60
PFTeDA	4.90	4.90	4.81	4.90	5.21
NMeFOSAA	9.80	9.80	9.62	9.80	10.42
NEtFOSAA	4.90	4.90	4.81	4.90	5.21
PFBS	632.30	637.15	620.29	719.53	677.98
PFPeS	776.39	822.24	826.92	916.51	784.28
PFHxS	3778.59	3700.21	3588.08	4556.16	4022.85
PFHpS	1206.67	1065.32	1267.34	1197.96	1148.08
PFOS	25999.23	28281.86	25086.52	28564.80	26114.84
PFNS	40.17	42.10	41.89	4.90	33.67
PFDS	2.45	2.45	2.40	2.45	2.60
4:2FTS	6.60	5.66	3.22	2.45	2.60
6:2FTS	755.27	250.42	40.17	12.25	13.02
8:2FTS	39.94	13.76	2.77	2.45	2.60

Table A6. PFAS data from BiPO4/UV Treatment of IDW, treated already with BOHP/UV, from Former Wurtsmith Site (Units: ppt)

Irradiation Time (min)	0.00	6.48	12.96	25.92	38.88
PFBA	224.13	148.13	109.37	112.55	209.81
PFPeA	132.63	173.89	97.74	79.82	127.16
PFHxA	188.78	194.71	116.93	91.88	162.39
PFHpA	153.81	132.84	88.70	63.67	172.57
PFOA	326.35	221.84	133.75	82.19	289.65
PFNA	3.64	5.21	2.49	7.14	4.92
PFDA	3.12	3.91	4.03	3.57	3.68
PFUnA	8.93	7.81	8.06	7.14	7.35
PFDoA	4.46	3.91	4.03	3.57	3.68
PFTrDA	4.46	3.91	4.03	3.57	3.68
PFTeDA	8.93	7.81	8.06	7.14	7.35
NMeFOSAA	17.86	15.63	16.13	14.29	14.71
NEtFOSAA	8.93	7.81	8.06	7.14	7.35
PFBS	5.95	5.27	4.45	4.99	5.34
PFPeS	19.14	13.49	9.20	9.53	12.31
PFHxS	250.96	243.41	183.26	195.98	233.39
PFHpS	39.57	28.47	16.30	13.21	18.48
PFOS	764.92	739.30	410.74	180.84	197.03
PFNS	8.93	7.81	8.06	7.14	7.35
PFDS	4.46	3.91	4.03	3.57	3.68
4:2FTS	4.46	3.91	4.03	3.57	3.68
6:2FTS	22.32	19.53	20.16	17.86	18.38
8:2FTS	4.46	3.91	4.03	3.57	3.68

Table A7. PFAS data from BiPO4/UV Treatment of IDW, treated already with BOHP/UV, from Willow Grove Site (Units: ppt)

Irradiation Time (min)	0.00	6.48	12.96	25.92	38.88
PFBA	430.86	236.89	135.30	165.32	127.41
PFPeA	113.85	92.24	57.17	55.96	61.27
PFHxA	96.81	99.19	67.28	72.31	71.17
PFHpA	72.10	79.24	51.14	57.68	51.73
PFOA	351.16	204.78	121.97	110.90	90.47
PFNA	12.94	6.38	3.09	5.56	1.34
PFDA	4.91	1.70	2.78	2.78	2.55
PFUnA	6.25	5.43	5.56	5.56	5.10
PFDoA	3.13	2.72	2.78	2.78	2.55
PFTrDA	3.13	2.72	2.78	2.78	2.55
PFTeDA	6.25	5.43	5.56	5.56	5.10
NMeFOSAA	12.50	10.87	11.11	11.11	10.20
NEtFOSAA	6.25	5.43	5.56	5.56	5.10
PFBS	303.53	251.63	264.38	234.33	225.55
PFPeS	429.22	421.06	359.85	314.50	307.39
PFHxS	1558.10	1301.65	1214.31	1160.45	1113.94
PFHpS	454.28	386.39	413.77	277.35	224.15
PFOS	9675.11	7052.70	6407.18	4380.72	3166.88
PFNS	6.25	5.43	5.56	5.56	5.10
PFDS	3.13	2.72	2.78	2.78	2.55
4:2FTS	3.13	2.72	2.78	2.78	2.55
6:2FTS	15.63	13.59	13.89	13.89	12.76
8:2FTS	3.13	2.72	2.78	2.78	2.55

Supporting Figures

Figure A1. Photograph of the Photo-cat-L unit employed in this study.

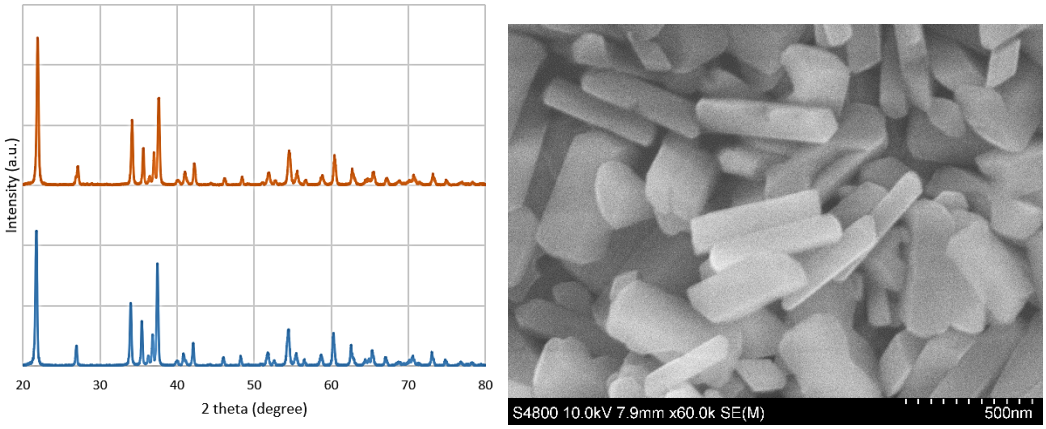

Figure A2. XRD pattern (left) and SEM image (right) of synthesized GaOOH.

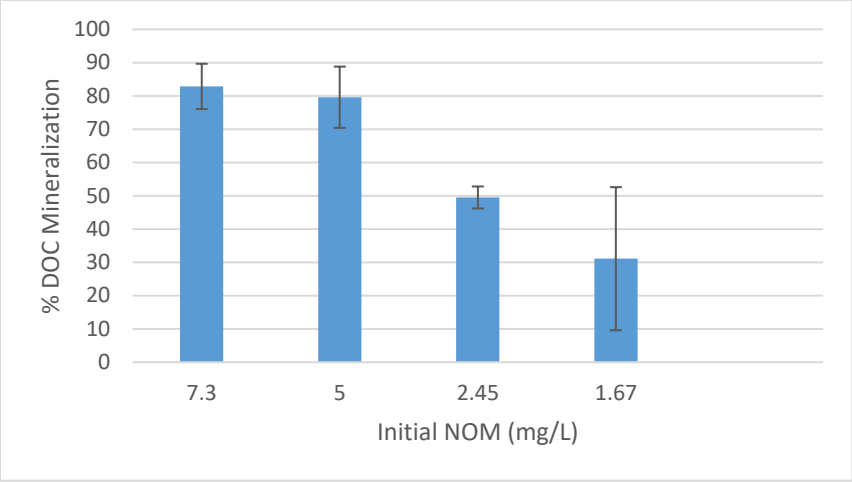

Figure A3. Percent degradation of NOM by BOHP/UV during PFOA experiments.

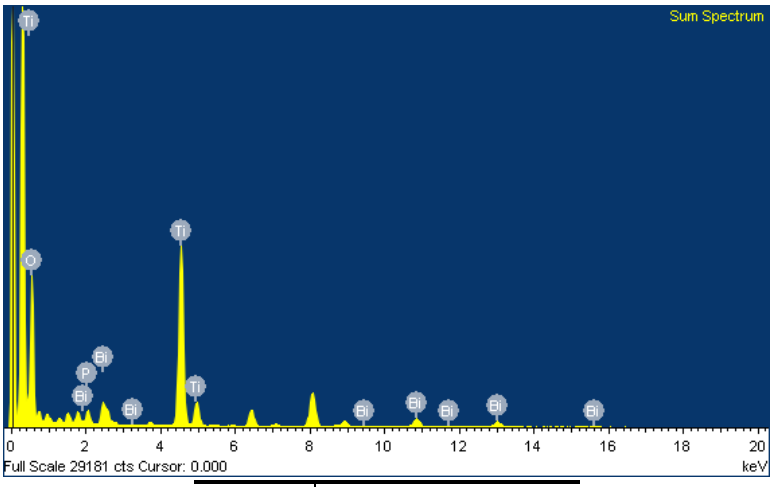

Element	Weight%	Atomic%
O K	31.73	62.47
P K	2.84	2.89
Ti K	48.88	32.14
Bi L	16.55	2.50
Totals	100.00	

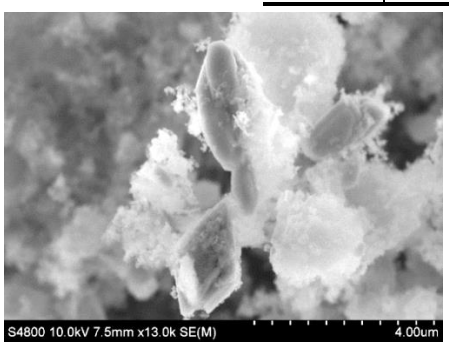

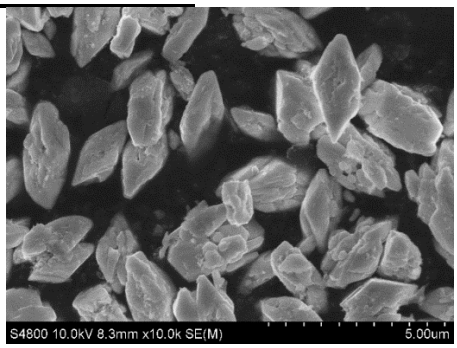

Figure A4. EDX analysis (top and middle) and SEM image (bottom left) of colloidal portion of recovered catalyst material, showing TiO_2 contamination surrounding BOHP microparticles. The settleable portion of the recovered BOHP is shown bottom right.

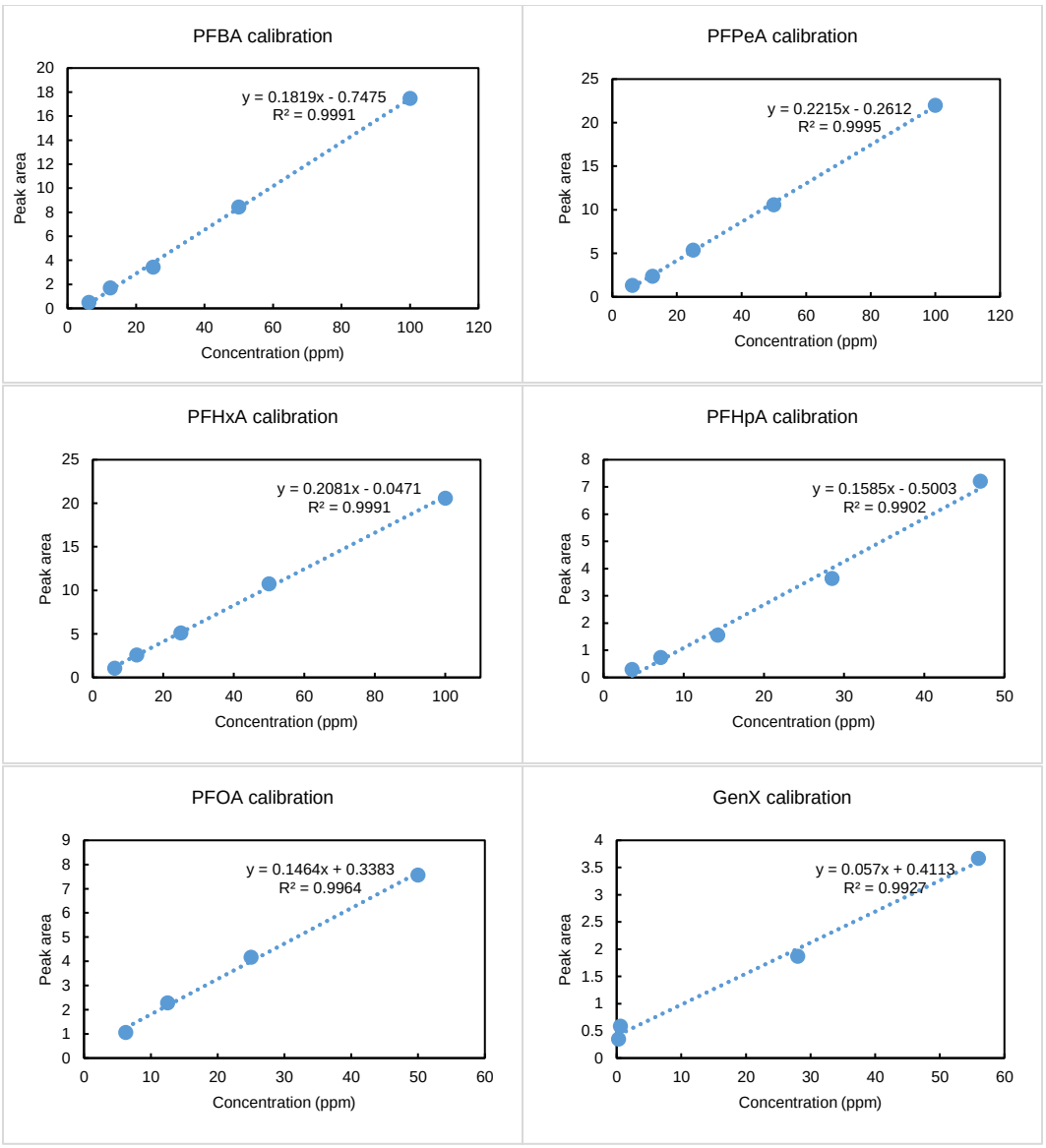

Figure A5. Example calibration curves used in in-house HPLC analyses of PFAS analytes for ppm-range experiments.

BATTELLE

Calibration Summary Report

Created with Analyst Reporter
Printed: 10/10/2019 12:28:46 PM

Analyte Name	PFHxA_1	**Data File**	AE_10092019_5-369.wiff
MRM Transition	313.0 / 269.0	**Result Table**	19-0863A
Internal Standard	13C5-PFHxA	**Instrument Name**	Triple Quad 6500+ Low Mass
Acquisition Date	10/9/2019 10:36:43 AM	**Acquisition Method**	5-369.dam

Regression Equation: y = 1.05710 x + 0.29191 (r = 0.99886) (weighting: 1 / x)

Vial	Sample Name	Sample ID	Used for ICAL	Target Conc. (ng/L)	Calculated Conc. (ng/L)	Recovery (%)
2	KR16	L1	True	101.00	86.77	85.9
3	KR17	L2	True	252.50	261.42	103.5
4	KR18	L3	True	505.00	524.84	103.9
5	KR19	L4	True	1010.00	998.90	98.9
6	KR20	L5	True	2525.00	2663.12	105.5
7	KR21	L6	True	10100.00	10697.07	105.9
8	KR22	L7	True	20200.00	19461.38	96.3

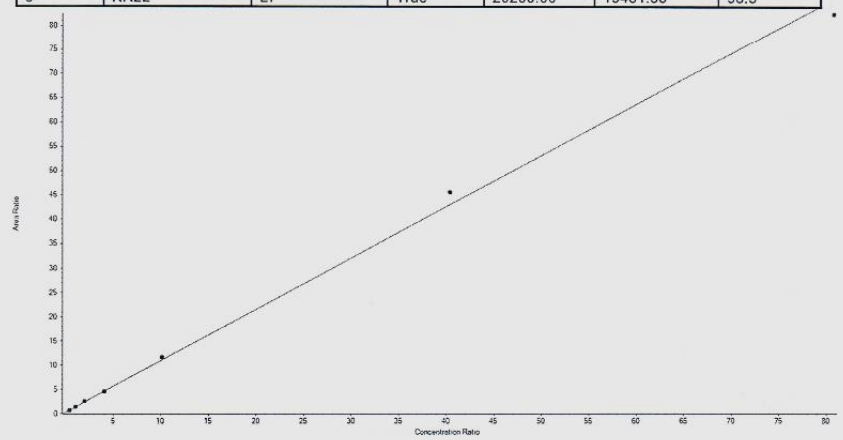

Analyte Name	PFOA_1	**Data File**	AE_10092019_5-369.wiff
MRM Transition	413.0 / 369.0	**Result Table**	19-0863A
Internal Standard	13C8-PFOA	**Instrument Name**	Triple Quad 6500+ Low Mass
Acquisition Date	10/9/2019 10:36:43 AM	**Acquisition Method**	5-369.dam

Regression Equation: y = 1.10158 x + -0.02447 (r = 0.99947) (weighting: 1 / x)

Vial	Sample Name	Sample ID	Used for ICAL	Target Conc. (ng/L)	Calculated Conc. (ng/L)	Recovery (%)
2	KR16	L1	True	100.00	107.33	107.3
3	KR17	L2	True	250.00	254.85	101.9
4	KR18	L3	True	500.00	489.99	98.0
5	KR19	L4	True	1000.00	1005.06	100.5
6	KR20	L5	True	2500.00	2243.21	89.7
7	KR21	L6	True	10000.00	10250.10	102.5
8	KR22	L7	True	20000.00	19999.46	100.0

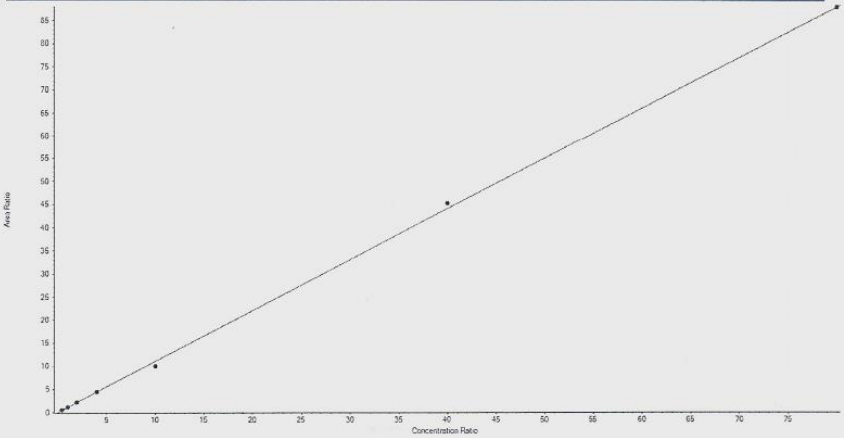

Figure A6. Example LC-MS/MS calibration data provided by Battelle, use in analyses of IDW samples.

Works Cited

1. Sahu, S. P.; Qanbarzadeh, M.; Ateia, M.; Torkzadeh, H.; Maroli, A. S.; Cates, E. L., Rapid Degradation and Mineralization of Perfluorooctanoic Acid by a New Petitjeanite Bi3O(OH)(PO4)2 Microparticle Ultraviolet Photocatalyst. *Environmental Science & Technology Letters* **2018,** *5*, (8), 533-538.